2023

Biophysical Interactions Control the Progression of Harmful Algal Blooms in Chesapeake Bay: A Novel Lagrangian Particle Tracking Model with Mixotrophic Growth and Vertical Migration

Jilian Xiong

Jian Shen

Qubin Qin

Michelle C. Tomlinson

Yinglong J. Zhang

See next page for additional authors

Original Publication Citation

Xiong, J., Shen, J., Qin, Q., Tomlinson, M. C., Zhang, Y. J., Cai, X., Ye, F., Cui, L., & Mulholland, M. R. (2023). Biophysical interactions control the progression of harmful algal blooms in Chesapeake Bay: A novel Lagrangian particle tracking model with mixotrophic growth and vertical migration. *Limnology and Oceanography Letters*, 1-11. https://doi.org/10.1002/lol2.10308

LIMNOLOGY AND OCEANOGRAPHY
Letters

ASLO
Open Access

Limnology and Oceanography Letters 2023

doi: 10.1002/lol2.10308

LETTER

Biophysical interactions control the progression of harmful algal blooms in Chesapeake Bay: A novel Lagrangian particle tracking model with mixotrophic growth and vertical migration

Jilian Xiong [1a*] *Jian Shen* [1] *Qubin Qin* [1] *Michelle C. Tomlinson* [2] *Yinglong J. Zhang* [1] *Xun Cai* [1,3] *Fei Ye* [1] *Linlin Cui* [1] *Margaret R. Mulholland* [4]

[1]Virginia Institute of Marine Science, William & Mary, Gloucester Point, Virginia; [2]National Centers for Coastal Ocean Science, National Oceanic and Atmospheric Administration, Silver Spring, Maryland; [3]ORISE Research Participation Program at EPA, Chesapeake Bay Program Office, Annapolis, Maryland; [4]Department of Ocean and Earth Sciences, Old Dominion University, Norfolk, Virginia

Scientific Significance Statement

Harmful algal blooms (HABs) threaten human health, marine life, and coastal economies. Accurate prediction of HABs is still a challenge. Lagrangian particle tracking (LPT) is a popular tool to track algal blooms, yet most LPT models use passive particles to represent algae without considering their interactions with ambient environmental conditions, including water temperature, salinity, available light, and nutrient concentrations. To advance predictions of HABs, we developed a novel LPT-Biological (LPT-Bio) model that integrates the advantages of both Lagrangian and Eulerian approaches by incorporating algal dynamics (mixotrophic growth, respiration, and mortality), algal biomass change, and diel vertical migration (DVM), along the predicted transport trajectories. The model is fully controlled by environmental conditions while maintaining mass balance. The improved LPT-Bio model was applied to simulate the 2020 *Margalefidinium polykrikoides* bloom in the Chesapeake Bay and successfully captured bloom intensity/duration/spatial extent and resolved locally aggregated patchiness. We found that capturing DVM patterns and including mixotrophic growth are critical for HAB simulation. The present model framework can provide a basis for developing a forecast system for HABs in the Bay.

Abstract

Climate change and nutrient pollution contribute to the expanding global footprint of harmful algal blooms. To better predict their spatial distributions and disentangle biophysical controls, a novel Lagrangian particle

*Correspondence: jxiong@vims.edu, xiongjilian@gmail.com

[a]Present address: University of Washington, School of Oceanography, Seattle, Washington

Associate editor: Raphael Kudela

Author Contribution Statement: JX and JS developed the research questions and designed the study approach. JX developed the biological particle tracking model and conducted data analysis. QQ provided advice on incorporating the biological processes into the particle tracking model. MCT guided analysis of satellite data. YJZ, XC, FY, and LC provided advice on numerical model computation. MRM assisted the interpretation of bloom observations. JX drafted the initial manuscript and all authors contributed to the interpretation of results and manuscript revisions.

Data Availability Statement: Data and metadata are available in the GitHub repository: https://github.com/Jilian0717/LPT-Bio_model.

Additional Supporting Information may be found in the online version of this article.

tracking and biological (LPT-Bio) model was developed with a high-resolution numerical model and remote sensing. The LPT-Bio model integrates the advantages of Lagrangian and Eulerian approaches by explicitly simulating algal bloom dynamics, algal biomass change, and diel vertical migrations along predicted trajectories. The model successfully captured the intensity and extent of the 2020 *Margalefidinium polykrikoides* bloom in the lower Chesapeake Bay and resolved fine-scale structures of bloom patchiness, demonstrating a reliable prediction skill for 7–10 d. The fully coupled LPT-Bio model initialized/calibrated by remote sensing and controlled by ambient environmental conditions appeared to be a powerful approach to predicting transport pathways, identifying bloom hotspots, resolving concentration variations at subgrid scales, and investigating responses of HABs to changing environmental conditions and human interference.

Harmful algal blooms (HABs) are increasing globally, posing an increasing threat to public and ecosystem health and coastal economies (Anderson et al. 2012; Glibert 2020). Climate change and escalating nutrient pollution contribute to the expanding footprint of HABs (Glibert 2020). A better understanding of the fundamental processes causing blooms to form and more accurate predictions of HABs and their responses to changing ocean conditions depend on developing new monitoring and laboratory techniques and numerical modeling (Anderson et al. 2012). Fueled by the increased frequency and geographic coverage of observational data, many approaches to formulating HAB models have been established (Franks 2018), including conceptual, statistical, and process-based/mechanistic models (McGillicuddy Jr 2010; Anderson et al. 2015; Ralston and Moore 2020).

Among techniques used to simulate HABs, Lagrangian particle tracking (LPT) is proving to be a powerful tool for identifying sites of HAB initiations, transport pathways, and dispersion patterns in coastal regions (Onitsuka et al. 2010; Velo-Suárez et al. 2010; Giddings et al. 2014; Gillibrand et al. 2016; Pinto et al. 2016; Weisberg et al. 2019; Lim et al. 2021). Combined with monitoring and hydrodynamic numerical modeling, LPT models are potential tools for HAB early warning (Wynne et al. 2013; Cusack et al. 2016; Davidson et al. 2021). LPT models are initiated by introducing numerical particles into a system and instructing them to be transported passively through physical processes. Most previous studies use these models to represent the transport of harmful algae without considering algal bloom dynamics, algal cell behaviors, or other environmental factors affecting algal growth. The prediction accuracy of these applications needs to be interpreted with caution since, while transported as particles, algal blooms are also highly regulated by ambient environmental conditions, that is, different algal species have growth optima and respond to environmental conditions favorable for their proliferation.

Several LPT models have imparted particles with behaviors/responses consistent with the organism of interest's biology and behavioral characteristics, for example, temperature-, salinity-, and light-regulated growth (Aleynik et al. 2016; Gillibrand et al. 2016; Zhou et al. 2021), and vertical migrations (Henrichs et al. 2015). Yet, no LPT models to date have incorporated nutrient limitation and mixotrophic growth, factors that may contribute to the competitive success of dinoflagellate groups (Mulholland et al. 2018; Hofmann et al. 2021; Qin et al. 2021). To better predict distributions of harmful algae and their response to the changing environment as they are transported to connected waterways and to disentangle biophysical controls, we developed a novel LPT and biological (LPT-Bio) model that integrates the complex growth strategies of mixotrophic dinoflagellates with physico-chemical environmental factors and coupled that with an advanced high-resolution numerical hydrodynamic model and remote sensing. The LPT-Bio model explicitly simulates algal growth, respiration, mortality, and diel vertical migration (DVM) patterns along the predicted transport trajectories.

Blooms of the harmful algal species *Margalefidinium polykrikoides* have become a global concern and the geographical distributions extend to coastal areas worldwide (Iwataki et al. 2008; Kudela and Gobler 2012; Al-Azri et al. 2014; López-Cortés et al. 2019; Roselli et al. 2020; Yñiguez et al. 2021). Nearly annual late summer blooms of *M. polykrikoides* in the Chesapeake Bay (CB) threaten many fisheries and aquaculture industries (Hudson 2018). Blooms of *M. polykrikoides* have expanded from those first-described in the York River (Mackiernan 1968) to those reported later in the mainstem and lower CB tributaries (Marshall and Egerton 2009; Mulholland et al. 2009; Morse et al. 2011, 2013).

In the late summer of 2020, high chlorophyll *a* (Chl *a*) concentrations were evident in the lower CB and the adjacent Atlantic Ocean based on Ocean Land Color Imager Level 3 products. Several coastal and CB monitoring programs confirmed the bloom to be *M. polykrikoides*. Satellite images recorded the complete bloom cycle, including the uncommon phenomenon of *M. polykrikoides* export from the lower CB to coastal Atlantic waters following Tropical Storm (TS) Isaias (Xiong et al. 2022). A similar expansion was only reported in 2007 (Mulholland et al. 2009) although the CB outflow plume persistently delivers materials toward the Atlantic Ocean (Jiang and Xia 2016). Currently, no model exists to accurately predict the trajectory and extent of *M. polykrikoides* in the CB and the adjacent continental shelf once a bloom has initiated. The extensive long-term observations and recent research parameterizing the key physiological processes and behavioral strategies of the regional *M. polykrikoides* (Hofmann et al. 2021; Qin et al. 2021) make the lower CB an ideal test

bed for validating the prediction ability of the LPT-Bio model. The advent of high-resolution daily ocean color imagery covering the CB region and the adjacent continental shelf (Wynne et al. 2021) further provides a unique opportunity to study HABs by merging the LPT-Bio model with satellite data. The newly developed LPT-Bio model and the successful simulation of the 2020 bloom demonstrate the predictive potential for HABs in the CB.

Methodology

Bloom monitoring

Surveillance data for the 2020 *M. polykrikoides* bloom include dataflow data, fixed site observations, water sample collections, and satellite imagery. The dataflow mappings and continuous measurements of Chl *a* at one fixed site inside bloom-impacted regions were collected by the Hampton Roads Sanitation District. The cell counts and species identifications via water samplings were made using standard microscopic methods at Old Dominion University and Virginia Institute of Marine Science and were reported to the Virginia Department of Health (VDH) for inclusion on the algal bloom surveillance map (https://www.vdh.virginia.gov/waterborne-hazards-control/algal-bloom-surveillance-map/).

The satellite-based daily monitoring, at 300 m resolution, was derived from Copernicus Sentinel-3 satellite data from the European Organisation for the Exploitation of Meteorological Satellites (EUMETSAT) and processed by NOAA's National Centers for Coastal Ocean Science (https://coastwatch.noaa.gov/cw_html/NCCOS.html). The satellite-derived Chl *a* were determined by a near-infrared to red ratio (Gilerson et al. 2010; Wynne et al. 2021) and the satellite-derived Red Band Difference (RBD) was used as a proxy of relative chlorophyll fluorescence to highlight areas with high algal biomass (Wolny et al. 2020; Jordan et al. 2021).

LPT-Bio model

Numerical particles were used to represent *M. polykrikoides* cells and were equipped with a virtual sensor to record varying cell densities driven by physical and biological processes. The horizontal and vertical locations of particles are (Chiu et al. 2018)

$$X^{n+1} = X^n + \left(U + \frac{\partial K_x}{\partial x}\right)\Delta t + R\sqrt{6K_x\Delta t}, \quad (1)$$

$$Y^{n+1} = Y^n + \left(V + \frac{\partial K_y}{\partial y}\right)\Delta t + R\sqrt{6K_y\Delta t}, \quad (2)$$

$$Z^{n+1} = Z^n + \left(W + \frac{\partial K_z}{\partial z} + W_{\text{swim}}\right)\Delta t + R\sqrt{6K_z\Delta t}, \quad (3)$$

where U, V, and W are velocities in Cartesian coordinates x, y, and z. R is a real random number with a zero mean and a uniform distribution between -1 and 1. K_x, K_y, and K_z are turbulent diffusion coefficients. W_{swim} is the daytime (06 : 00–18 : 00) ascent and nighttime (18 : 00–06 : 00) descent velocity (Park et al. 2001). We integrated algal bloom dynamics (i.e., mixotrophic growth, respiration, temperature-modulated mortality, and density-related aggregation settling) into the LPT-Bio model to simulate cell density variations, which are dynamically driven by environmental parameters (i.e., temperature, salinity, irradiance, and nutrients). The cell density (C_i^t) recorded by particle i is controlled by

$$\frac{dC_i^t}{dt} = (G - \text{Res} - M_T)C_i^t - M_{\text{agg}}, \quad (4)$$

where G is the mixotrophic growth rate, including phototrophic (G_o^P) and heterotrophic growth (G_o^H). The phototrophic growth is

$$G_o^P = G_{\text{opt}}^P f(T) f(S) \min[f(I), f(DIN)], \quad (5)$$

where G_{opt}^P is the phototrophic growth rate at optimal conditions. $f(T)$, $f(S)$, $f(I)$, and $f(DIN)$ are temperature-, salinity-, irradiance-, and DIN-limited functions, respectively. Details for limitation functions are given in Qin et al. (2021).

The heterotrophic growth is

$$G_o^H = G_{\text{opt}}^H f(T) f(S) f(\text{OM}_{12}), \quad (6)$$

where G_{opt}^H is the maximum heterotrophic growth rate at optimal conditions. The growth-limiting function for the bioavailable organic matter (DOM and POM smaller than 12 μm, Jeong et al. 2004), $f(\text{OM}_{12})$, is adjusted based on bloom intensities (Supporting Information Table S1).

Without considering interactions between phototrophy and heterotrophy, the mixotrophic growth rate equals the heterotrophic growth rate at night and consists of phototrophy and heterotrophy during the daytime and cannot exceed the maximum growth rate at a certain temperature and salinity (Qin et al. 2021). The mixotrophic growth rate is thus

$$G = \begin{cases} \min\left[G_o^H + G_o^P,\ G_{\text{opt}}^P f(T) f(S)\right], & \text{Daytime} \\ G_o^H, & \text{Nighttime} \end{cases}. \quad (7)$$

The cell density loss terms in Eq. (4) include respiration (Res, Qin et al. 2021), temperature-modulated mortality (M_T, Hofmann et al. 2021), and density-related aggregation settling ($M_{\text{agg}} = \tau\left(C_i^t\right)^2$, $\tau = 0.1$ [cells m^{-3} d]$^{-1}$ is the aggregation parameter; Lima and Doney 2004).

The high-resolution unstructured-grid model SCHISM (Zhang et al. 2016; Supporting Information Fig. S1) was utilized to provide 3D velocities, temperature, salinity, and near-surface irradiance to drive particle transport and cell density variations. Blooms of *M. polykrikoides* are usually patchy with

local accumulations due to algal behavior and physical transport. The superior boundary fitting and local refinement enable unstructured-grid models to perform better in regions with complex bathymetry and shoreline geometry (Nunez et al. 2020). The present hydrodynamic model did not activate the wave module, yet wave effects, for example, wave-induced sea surface roughness and Stokes drift advection, are suggested to be important factors impacting simulated particle trajectories, especially during wind events (Mao and Xia 2020). Moreover, nutrient and turbidity data associated with algal growth were from Chesapeake Bay Program (CBP) monitoring data (https://data.chesapeakebay.net/WaterQuality; Fig. 1).

LPT-Bio model simulations

The initial particle seeding locations and total particle numbers were determined by satellite-derived Chl *a* (mg Chl *a* m^{-3}), which were converted into cell density (cells m^{-3}) using a conversion factor of 1.69×10^{-8} mg Chl *a* $cell^{-1}$ for *M. polykrikoides* (Hofmann et al. 2021). Satellite-derived RBD values identify locations with high algal biomass, and pixels with RBD greater than 2.00×10^{-4} in the lower CB were chosen as particle-releasing regions (Supporting Information Fig. S2). Particle numbers within selected pixels were determined as the ratio of satellite-derived cell density to the initial cell density of each particle, C_0 (cells m^{-3} $particle^{-1}$). $C_0 = 1.00 \times 10^7$ cells m^{-3} $particle^{-1}$ was chosen to balance the computational cost and model robustness. The sensitivity of simulated Chl *a* to C_0 is presented in Supporting Information Figs. S3, S4. Particles were then seeded randomly inside selected pixels.

The *M. polykrikoides* bloom was first observed on 22 July 2020, in the lower James River and then observed outside the James River mouth 5 d later (Supporting Information Figs. S5, S6). Based on available high-quality satellite images, three dates (22 July, 28 July, and 08 August) were selected to release particles (i.e., as reinitializations), with the tracking periods ranging from 7 to 10 d. The total released particles were 76,809, 120,448, and 325,841, respectively (Supporting

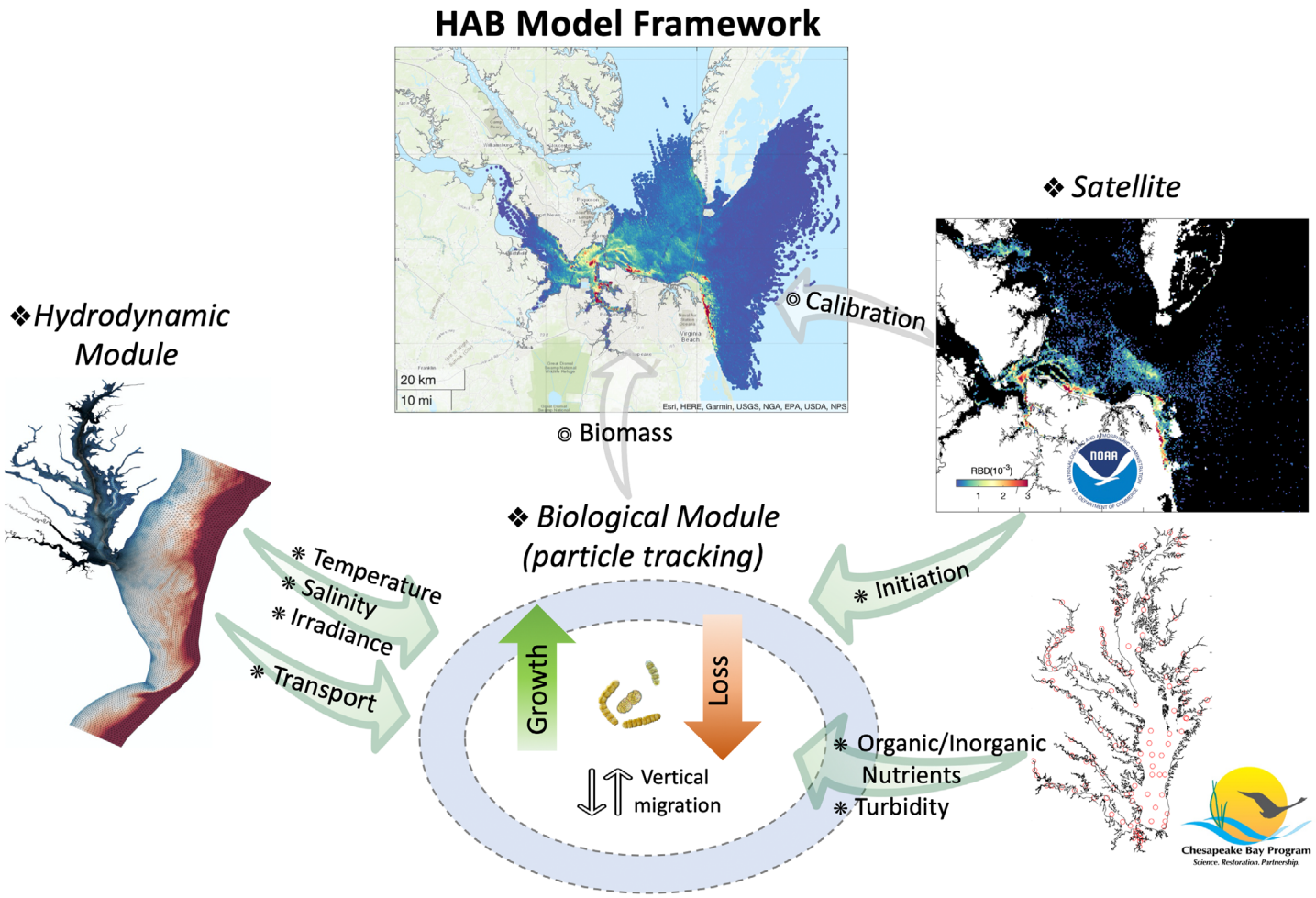

Fig. 1. HAB model framework that includes three components: hydrodynamic module of SCHISM, biological module based on LPT, and NOAA satellite datasets.

Information Table S1). The satellite overpass time was around 14 : 30–15 : 30 and particles were released at 15 : 00 at a depth of 0.5 m on the three dates. Each particle is implemented with DVMs with a daytime ascent rate of 30 m d^{-1} and a nighttime descent rate of 70 m d^{-1} (Sohn et al. 2011). Sensitivity simulations were performed to assess the importance of DVMs on bloom development.

To compare model results with satellite data, the simulated cell densities recorded by all particles in the same pixel (coordinates given by satellite images) were integrated together, then converted to Chl *a*, and saved every half an hour. A best-match strategy was applied to assess model performance given the inherent uncertainties in satellite and model configurations. The closest model-satellite pair with respect to Chl *a* for each pixel was searched between 10 : 00 and 18:00. The normalized Taylor diagram (Taylor 2001) was used to evaluate the model prediction skill, in terms of correlation coefficient, normalized centered root-mean-square difference, and normalized standard deviations of the model against satellite data (Hofmann et al. 2008).

Results and discussion

HAB development and progression

Satellite images revealed the progression of *M. polykrikoides* blooms from the lower James River to the lower CB and then

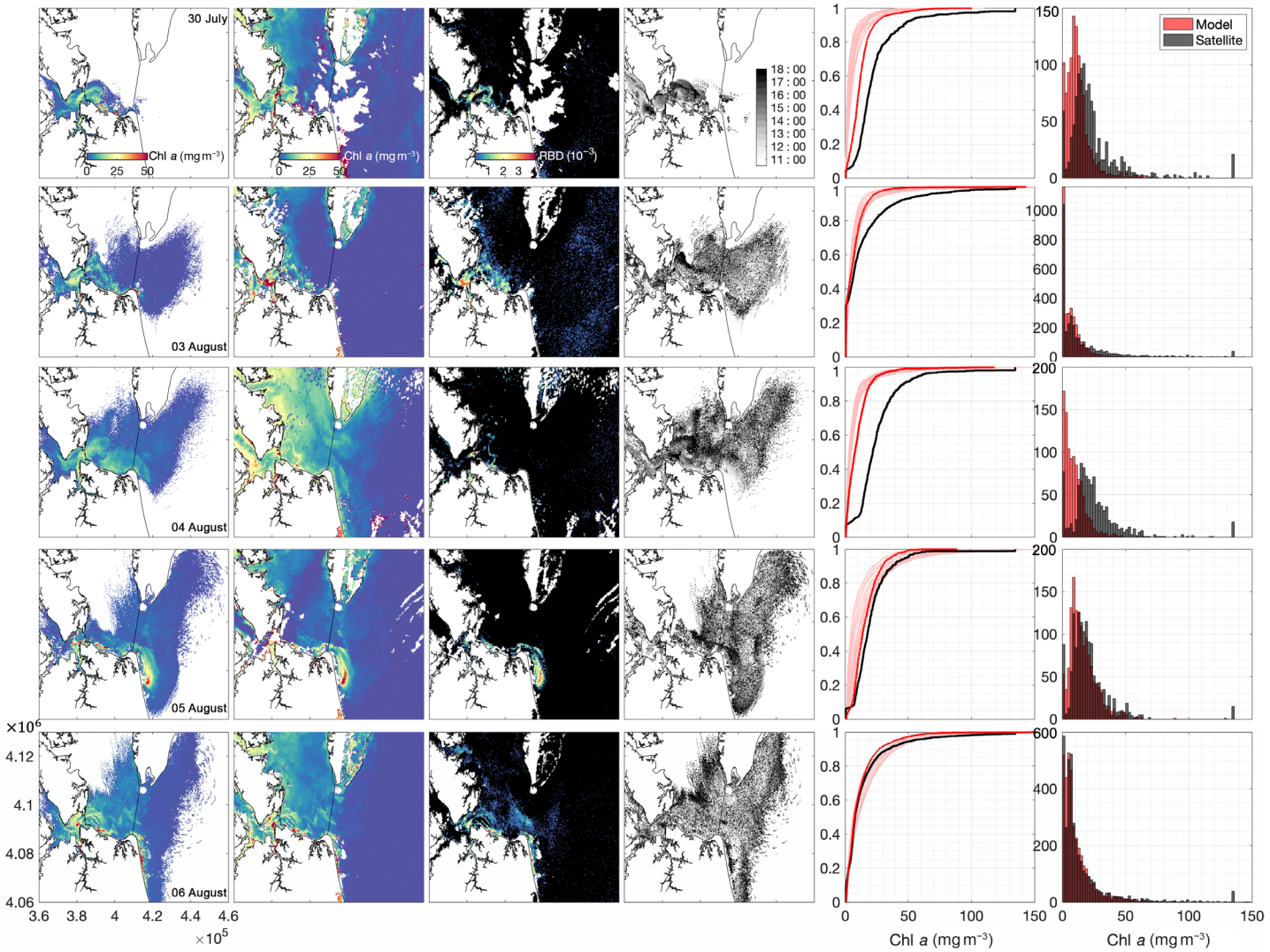

Fig. 2. Simulations with particles released on 28 July 2020. Column 1: simulated Chl *a* concentrations (Chl *a*, depth < 1 m); Column 2: satellite-derived Chl *a*; Column 3: satellite-derived RBD value; Column 4: best-match time determined daily between 10 : 00 and 18 : 00; Column 5: cumulative distribution function of simulated and satellite-derived Chl *a*. The black lines represent satellite data. The red lines are simulations of Chl *a* from the best-match searching, while faded red lines are simulations saved every half-hour between 10 : 00 and 18 : 00. Column 6: histogram of simulated (best-match) and satellite-derived Chl *a*.

coastal Atlantic waters (Fig. 2; Supporting Information Figs. S7, S8). The bloom first appeared in the lower James River on 22 July and subsequently propagated coastward, with a density of 7610 cells mL^{-1} (Supporting Information Fig. S6) measured on 27 July outside the James River mouth. A marked coastward progression and a massive bloom at Virginia Beach occurred after TS Isaias (Supporting Information Fig. S1) passed the CB watershed on 04 August. Cell densities reached 8640 cells mL^{-1} at the southern bank of the CB outside the James River mouth, and 6990 cells mL^{-1} were recorded at the Virginia Beach oceanfront on 06 August following the storm (Supporting Information Fig. S6), resulting in discolored and foul-smelling waters. The dataflow mappings and satellite images indicate the spatial patchiness of the bloom, while fixed site Chl *a* measurements show marked temporal variations in bloom intensity (Supporting Information Fig. S5). Although *M. polykrikoides* blooms occur almost annually in the lower CB and its tributaries, export to the Atlantic Ocean has only been reported in 2007 (Mulholland et al. 2009), 2020, and 2021 (https://www.vdh.virginia.gov/waterborne-hazards-control/algal-bloom-surveillance-map/).

LPT-Bio model results

Evolutions of cell concentrations and coastward transport of HABs from the James River to the lower CB and coastal Atlantic waters were well-captured by the LPT-Bio model (Fig. 2), despite some biases in bloom intensity and extent; a good model performance was achieved (on 05 and 06 August) with correct reproduction of the massive bloom at Virginia Beach (Fig. 2). The dense bloom streaks at the James River mouth were also well reproduced (Fig. 2; Supporting Information Fig. S8). The LPT-Bio model generally predicts more

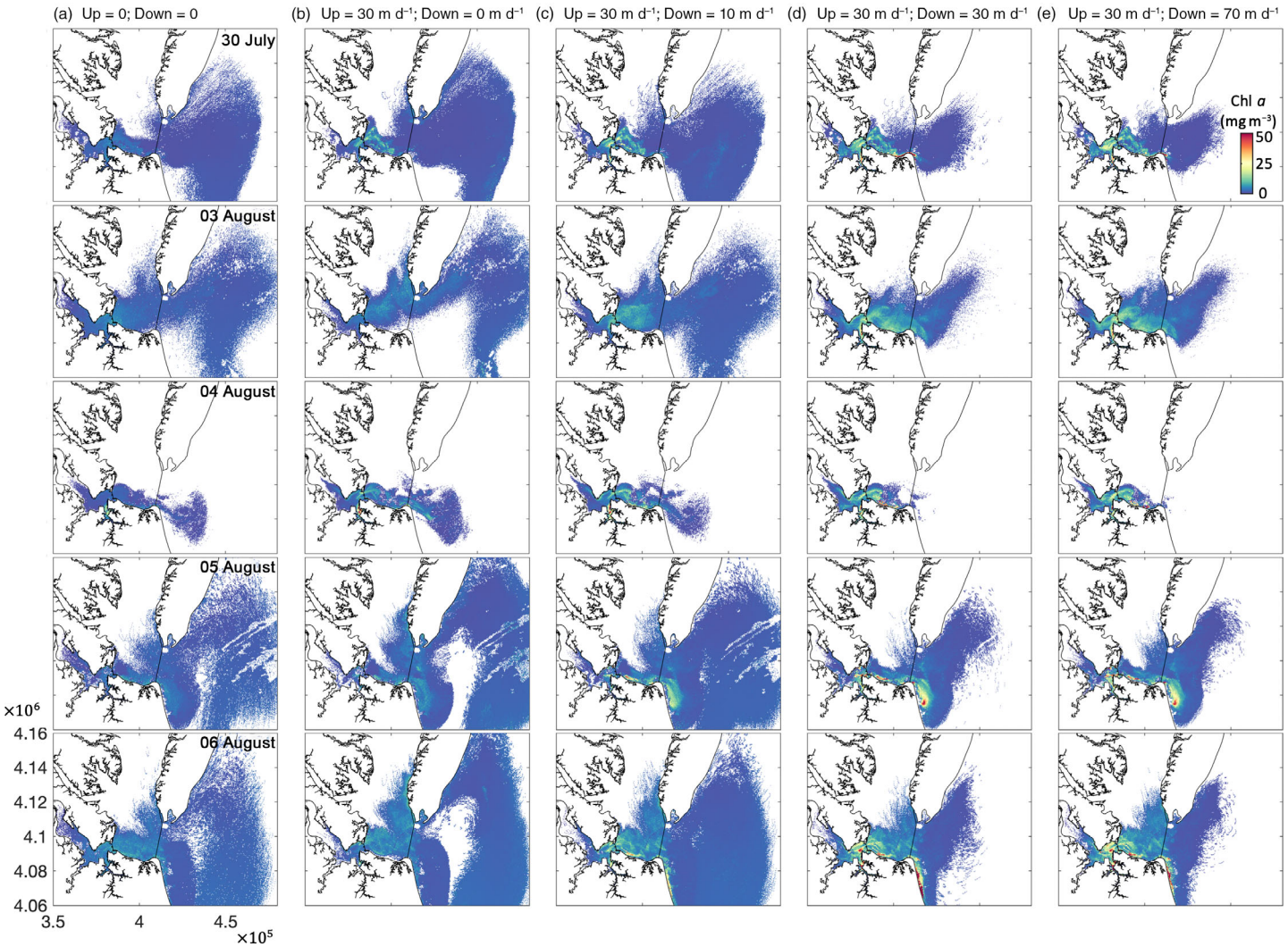

Fig. 3. Simulated Chl *a* (depth < 1 m) with different DVM speeds. Particles were released on 28 July 2020. The vertical migration speeds were annotated above each column.

accurately when transport processes dominate the bloom proliferation, that is, the best performance was achieved after the passage of TS Isaias when physical processes dominated bloom transport (Supporting Information Fig. S9). The quantitative comparisons between the LPT-Bio model and satellite images are shown in Supporting Information Fig. S9, where most data points cluster within the 0.5–1.0 normalized centered root-mean-square circle and the 0.5–1.0 normalized standard deviation circle. The average model-data correlation coefficient for all comparison dates is 0.58 (Supporting Information Table S2). In terms of simulating Chl *a* in the CB, the LPT-Bio model skill is comparable to other 3D biogeochemical models (Yu and Shen 2021). Since ocean color images cannot differentiate the chlorophyll signal from *M. polykrikoides* and other co-occurring phytoplankton groups, the simulated Chl *a* specific to *M. polykrikoides* is generally smaller than the satellite-derived Chl *a* (Fig. 2, Columns 5–6; Supporting Information Figs. S7, S8). Overall, the model demonstrated a reliable predictive ability over the 7- to 10-d period when the 2020 *M. polykrikoides* bloom initiated and was transported to the coast. Once a bloom initiation has been identified through coastal monitoring programs, the LPT-Bio model, incorporated into a hydrodynamic and water quality forecast system, can predict bloom transport trajectories, intensities, and variations.

Effects of DVMs

M. polykrikoides vertically migrates with daytime ascents and nighttime descents, as do other dinoflagellates (Park et al. 2001; Jeong et al. 2015; Noh et al. 2018). DVMs are thought to optimize cell exposure to high concentrations of near-surface sunlight during the day and high concentrations of near-bottom nutrients at night where they might also avoid predators (Jeong et al. 2015). Here, we suggest that DVMs may also allow fast-swimming algae to circumvent physical washout due to coastal ocean circulation and thereby achieve high cell densities as observed in the lower CB (Fig. 3). Particles released on 28 July were used to evaluate DVMs because the best model performance was achieved during this tracking period. Without DVMs, the passive particles were transported by currents, leading to a large-scale dispersal of bloom organisms outside the bay mouth (Column 1 in Fig. 3). Under this scenario, the predicted Chl *a* remained low and almost no blooms developed. The model better reproduced cell abundances in surface waters after applying a daytime ascent term with a swimming speed of 30 m d^{-1} (Column 2 in Fig. 3). Employing both terms for daytime ascents and nighttime descents, the bloom organisms accumulated in the nearshore region and the simulated bloom aggregations better matched observations (Columns 3–5 in Fig. 3). The vertical migration speed applied here is sufficient to create the bloom intensity in shallow regions, although algal cells might adjust their swimming behaviors based on phototaxis, geotaxis, temperature, turbulence intensity, stratification, internal biochemical state, chain length, life-cycle stage, and so on (Heaney and Eppley 1981; Park et al. 2001; Erga et al. 2015; Henrichs et al. 2015; Lovecchio et al. 2019; Brosnahan et al. 2020; Shikata et al. 2020; Lim et al. 2022). More field observations and laboratory experiments are expected to better constrain the DVMs of *M. polykrikoides*. It is clear, however, as seen in our findings and earlier studies (Gillibrand et al. 2016; Qin et al. 2021) that vertical migrations are critical for bloom development and accumulations, especially in nearshore regions with strong flushing (Shulman et al. 2012).

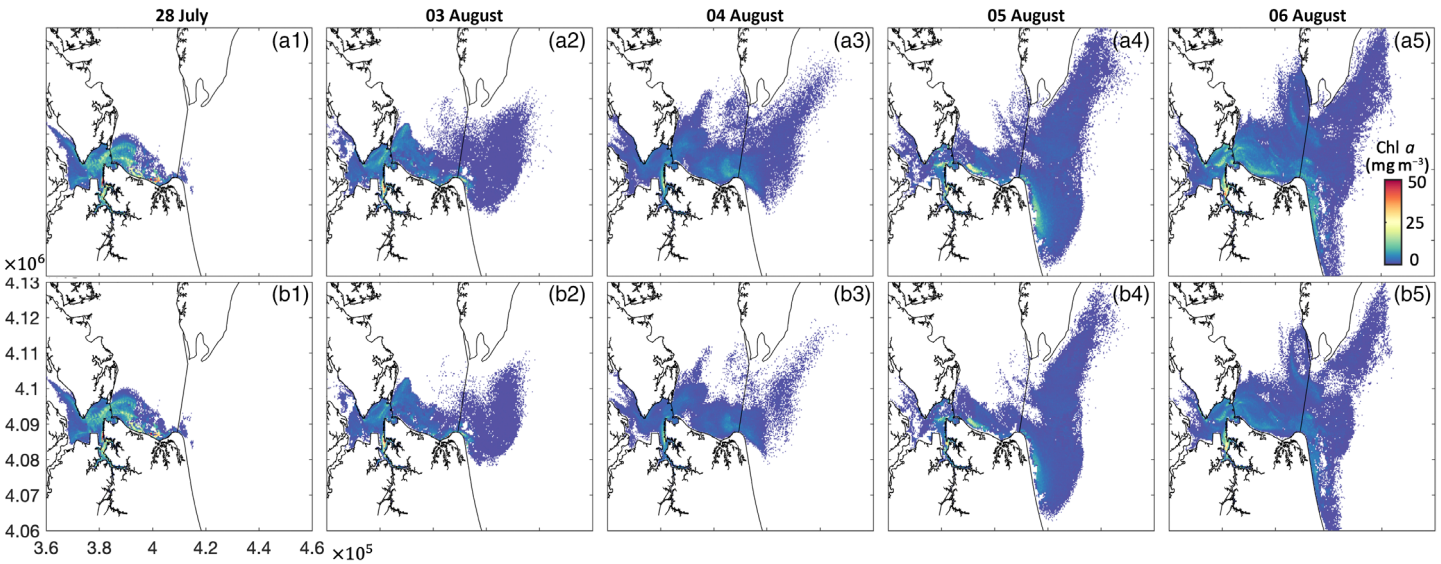

Fig. 4. Simulated Chl *a* concentrations (depth < 1 m) from sensitivity tests of mixotrophy and algal bloom dynamics with particles released on 28 July 2020, by disabling (**a1**–**a5**) heterotrophy and (**b1**–**b5**) all growth and biomass loss processes.

Necessity of incorporating mixotrophy and algal bloom dynamics into LPT models

The LPT models are useful for predicting the transport and spatial distributions of HABs (Fernandes-Salvador et al. 2021) and detecting bloom initiation sites (Zhang et al. 2020; Clark et al. 2021). In principle, the tracked particles could spread over the whole model domain if they are allowed to disperse randomly. Yet, only locations with favorable conditions can trigger bloom initiation since biological and environmental factors come into play. Bloom intensities and locations are highly related to environmental conditions, including temperature, salinity, available light, nutrient concentrations, and local transport conditions (Qin and Shen 2019).

To demonstrate the necessity of incorporating mixotrophy and algal bloom dynamics into LPT models, we first disabled the heterotrophic growth of *M. polykrikoides*, which can assimilate organic nutrients to likely outcompete other algal species (Mulholland et al. 2018) and found that the phototrophic growth alone cannot sustain the bloom intensities (Fig. 4). Although particles reached Virginia Beach after the storm (Fig. 4), the simulated Chl *a* concentrations were about 50% of the base scenario (Supporting Information Table S3), consistent with previous findings that the degree of heterotrophy significantly impacted the timing, duration, distribution, and magnitude of the *M. polykrikoides* bloom (Hofmann et al. 2021; Qin et al. 2021). A further decrease in bloom intensity was predicted when all growth (heterotrophy and phototrophy) and loss terms related to the bloom dynamics were disabled, that is, particles only carried the initial cell density without being modified during the tracking (Fig. 4). Therefore, fully coupling particle tracking models with algal bloom dynamics regulated by surrounding environmental factors is a must to accurately predict HABs, especially under changing climate conditions.

Conclusions

Individual-based modeling utilizing particle tracking techniques with implemented algal bloom dynamics offers a more accurate approach to simulating HABs. This type of model specifies algal behavior patterns and examines interactions between physical transport and biological processes. Here, we developed a novel LPT-Bio model with algal bloom dynamics driven by surrounding environmental parameters. The model was coupled with a high-resolution numerical hydrodynamic model and remote sensing. The satellite-derived Chl *a* was used to initialize and calibrate the LPT-Bio model. The physical transport and DVM parameterizations used in the model well captured the bloom intensity/patchiness, coastward expansion, and penetration into the Atlantic Ocean.

The relatively good model predictions of the 2020 *M. polykrikoides* bloom over the 7–10 d of its development and the full incorporation of environmental factors suggest that the present model framework may serve as the foundation for a HAB forecast system for *M. polykrikoides* blooms in the CB, as well as investigate responses of HABs to the changing ocean environments. Further improvements can be made in model configurations and monitoring sources, for example, the inclusion of cyst dynamics (Hofmann et al. 2021), and the availability of satellite data with a higher temporal resolution. The present modeling technique can be transferred to other motile organisms such as raphidophytes (Handy et al. 2005) or nonmotile algal species and water bodies if remote sensing (or synoptic bloom mappings) and parameterizations of cell physiological processes are available.

References

Al-Azri, A. R., S. A. Piontkovski, K. A. Al-Hashmi, J. I. Goes, H. D. R. Gomes, and P. M. Glibert. 2014. Mesoscale and nutrient conditions associated with the massive 2008 *Cochlodinium polykrikoides* bloom in the sea of Oman/Arabian gulf. Estuar. Coast. **37**: 325–338. doi:10.1007/s12237-013-9693-1

Aleynik, D., A. C. Dale, M. Porter, and K. Davidson. 2016. A high resolution hydrodynamic model system suitable for novel harmful algal bloom modelling in areas of complex coastline and topography. Harmful Algae **53**: 102–117.

Anderson, C. R., S. K. Moore, M. C. Tomlinson, J. Silke, and C. K. Cusack. 2015. Living with harmful algal blooms in a changing world: Strategies for modeling and mitigating their effects in coastal marine ecosystems, p. 495–561. *In*, *Coastal and marine hazards, risks, and disasters*. Elsevier.

Anderson, D. M., A. D. Cembella, and G. M. Hallegraeff. 2012. Progress in understanding harmful algal blooms: Paradigm shifts and new technologies for research, monitoring, and management. Ann. Rev. Mar. Sci. **4**: 143–176.

Brosnahan, M. L., A. D. Fischer, C. B. Lopez, S. K. Moore, and D. M. Anderson. 2020. Cyst-forming dinoflagellates in a warming climate. Harmful Algae **91**: 101728.

Chiu, C. M., C. J. Huang, L. C. Wu, Y. J. Zhang, L. Z. H. Chuang, Y. Fan, and H. C. Yu. 2018. Forecasting of oil-spill trajectories by using SCHISM and X-band radar. Mar. Pollut. Bull. **137**: 566–581.

Clark, S., K. A. Hubbard, D. J. McGillicuddy Jr., D. K. Ralston, and S. Shankar. 2021. Investigating *Pseudo-nitzschia australis* introduction to the Gulf of Maine with observations and models. Cont. Shelf Res. **228**: 104493.

Cusack, C., and others. 2016. Harmful algal bloom forecast system for SW Ireland. Part II: Are operational oceanographic models useful in a HAB warning system. Harmful Algae **53**: 86–101.

Davidson, K., and others. 2021. HABreports: Online early warning of harmful algal and biotoxin risk for the Scottish shellfish and finfish aquaculture industries. Front. Mar. Sci. **8**: 350.

Erga, S. R., C. D. Olseng, and L. H. Aarø. 2015. Growth and diel vertical migration patterns of the toxic dinoflagellate

Protoceratium reticulatum in a water column with salinity stratification: The role of bioconvection and light. Mar. Ecol. Prog. Ser. **539**: 47–64.

Fernandes-Salvador, J. A., and others. 2021. Current status of forecasting toxic harmful algae for the north-east Atlantic shellfish aquaculture industry. Front. Mar. Sci. **8**: 656.

Franks, P. J. 2018. Recent advances in modelling of harmful algal blooms, p. 359–377. *In*, *Global ecology and oceanography of harmful algal blooms*. Springer.

Giddings, S. N., and others. 2014. Hindcasts of potential harmful algal bloom transport pathways on the Pacific northwest coast. J. Geophys. Res. Oceans **119**: 2439–2461.

Gilerson, A. A., A. A. Gitelson, J. Zhou, D. Gurlin, W. Moses, I. Ioannou, and S. A. Ahmed. 2010. Algorithms for remote estimation of chlorophyll-a in coastal and inland waters using red and near infrared bands. Opt. Express **18**: 24109–24125.

Gillibrand, P. A., B. Siemering, P. I. Miller, and K. Davidson. 2016. Individual-based modelling of the development and transport of a *Karenia mikimotoi* bloom on the North-west European continental shelf. Harmful Algae **53**: 118–134.

Glibert, P. M. 2020. Harmful algae at the complex nexus of eutrophication and climate change. Harmful Algae **91**: 101583.

Handy, S. M., K. J. Coyne, K. J. Portune, E. Demir, M. A. Doblin, C. E. Hare, S. C. Cary, and D. A. Hutchins. 2005. Evaluating vertical migration behavior of harmful raphidophytes in the Delaware Inland Bays utilizing quantitative real-time PCR. Aquat. Microb. Ecol. **40**: 121–132.

Heaney, S. I., and R. W. Eppley. 1981. Light, temperature and nitrogen as interacting factors affecting diel vertical migrations of dinoflagellates in culture. J. Plankton Res. **3**: 331–344.

Henrichs, D. W., R. D. Hetland, and L. Campbell. 2015. Identifying bloom origins of the toxic dinoflagellate *Karenia brevis* in the western Gulf of Mexico using a spatially explicit individual-based model. Ecol. Model. **313**: 251–258.

Hofmann, E., and others. 2008. Eastern US continental shelf carbon budget: Integrated models, data assimilation, and analysis. Oceanography **21**: 86–104.

Hofmann, E. E., J. M. Klinck, K. C. Filippino, T. Egerton, L. B. Davis, M. Echevarría, E. Pérez-Vega, and M. R. Mulholland. 2021. Understanding controls on *Margalefidinium polykrikoides* blooms in the lower Chesapeake Bay. Harmful Algae **107**: 102064.

Hudson, K. 2018, *Virginia shellfish aquaculture situation and outlook report. Results of the 2017 Virginia Shellfish Aquaculture Crop Reporting Survey (VIMS marine resource report). No. 2018-9. Virginia Sea Grant VSG-18-3*. Virginia Sea Grant Marine Extension Program, Virginia Institute of Marine Science.

Iwataki, M., H. Kawami, K. Mizushima, C. M. Mikulski, G. J. Doucette, J. R. Relox Jr., A. Anton, Y. Fukuyo, and K. Matsuoka. 2008. Phylogenetic relationships in the harmful dinoflagellate *Cochlodinium polykrikoides* (Gymnodiniales, Dinophyceae) inferred from LSU rDNA sequences. Harmful Algae **7**: 271–277.

Jeong, H. J., Y. D. Yoo, J. S. Kim, T. H. Kim, J. H. Kim, N. S. Kang, and W. Yih. 2004. Mixotrophy in the phototrophic harmful alga *Cochlodinium polykrikoides* (Dinophycean): Prey species, the effects of prey concentration, and grazing impact. J. Eukaryot. Microbiol. **51**: 563–569.

Jeong, H. J., and others. 2015. A hierarchy of conceptual models of red-tide generation: Nutrition, behavior, and biological interactions. Harmful Algae **47**: 97–115.

Jiang, L., and M. Xia. 2016. Dynamics of the Chesapeake Bay outflow plume: Realistic plume simulation and its seasonal and interannual variability. J. Geophys. Res. Oceans **121**: 1424–1445. doi:10.1002/2015JC011191

Jordan, C., and others. 2021. Using the red band difference algorithm to detect and monitor a Karenia spp. bloom off the south coast of Ireland. Front. Mar. Sci. **8**: 638889.

Kudela, R. M., and C. J. Gobler. 2012. Harmful dinoflagellate blooms caused by *Cochlodinium* sp.: Global expansion and ecological strategies facilitating bloom formation. Harmful Algae **14**: 71–86.

Lim, Y. K., G. Lee, B. S. Park, H. Y. Cho, J. Y. Choi, and S. H. Baek. 2021. Differential responses of the dinoflagellate *Cochlodinium polykrikoides* bloom to episodic typhoon events. J. Appl. Phycol. **33**: 2299–2311.

Lim, Y. K., J. H. Kim, H. Ro, and S. H. Baek. 2022. Thermotaxic diel vertical migration of the harmful dinoflagellate *Cochlodinium* (*Margalefidinium*) polykrikoides: Combined field and laboratory studies. Harmful Algae **118**: 102315.

Lima, I. D., and S. C. Doney. 2004. A three-dimensional, multinutrient, and size-structured ecosystem model for the North Atlantic. Global Biogeochem. Cycles **18**: GB3019. doi:10.1029/2003GB002146

López-Cortés, D. J., and others. 2019. The state of knowledge of harmful algal blooms of *Margalefidinium polykrikoides* (aka *Cochlodinium polykrikoides*) in Latin America. Front. Mar. Sci. **6**: 463.

Lovecchio, S., E. Climent, R. Stocker, and W. M. Durham. 2019. Chain formation can enhance the vertical migration of phytoplankton through turbulence. Sci. Adv. **5**: eaaw7879.

Mackiernan, G. B. (1968). Seasonal of dinoflagellates in the lower York River, Virginia. Master Thesis, College of William and Mary, Williamsburg, VA. 104 pp.

Mao, M., and M. Xia. 2020. Particle dynamics in the nearshore of Lake Michigan revealed by an observation-modeling system. J. Geophys. Res. Oceans **125**: e2019JC015765.

Marshall, H. G., and T. A. Egerton. 2009. Phytoplankton blooms: Their occurrence and composition within Virginia's tidal tributaries. Va. J. Sci. **60**: 3.

McGillicuddy, D. J., Jr. 2010. Models of harmful algal blooms: Conceptual, empirical, and numerical approaches. J. Mar. Syst. **83**: 105–107.

Morse, R. E., J. Shen, J. L. Blanco-Garcia, W. S. Hunley, S. Fentress, M. Wiggins, and M. R. Mulholland. 2011. Environmental and physical controls on the formation and transport of blooms of the dinoflagellate *Cochlodinium polykrikoides* Margalef in the lower Chesapeake Bay and its tributaries. Estuar. Coast. **34**: 1006–1025.

Morse, R. E., M. R. Mulholland, W. S. Hunley, S. Fentress, M. Wiggins, and J. L. Blanco-Garcia. 2013. Controls on the initiation and development of blooms of the dinoflagellate *Cochlodinium polykrikoides* Margalef in lower Chesapeake Bay and its tributaries. Harmful Algae **28**: 71–82.

Mulholland, M. R., and others. 2009. Understanding causes and impacts of the dinoflagellate, *Cochlodinium polykrikoides*, blooms in the Chesapeake Bay. Estuar. Coast. **32**: 734–747.

Mulholland, M. R., R. Morse, T. Egerton, P. W. Bernhardt, and K. C. Filippino. 2018. Blooms of dinoflagellate mixotrophs in a lower Chesapeake Bay tributary: Carbon and nitrogen uptake over diurnal, seasonal, and interannual timescales. Estuar. Coast. **41**: 1744–1765.

Noh, J. H., W. Kim, S. H. Son, J. H. Ahn, and Y. J. Park. 2018. Remote quantification of *Cochlodinium polykrikoides* blooms occurring in the East Sea using geostationary ocean color imager (GOCI). Harmful Algae **73**: 129–137.

Nunez, K., Y. J. Zhang, J. Herman, W. Reay, and C. Hershner. 2020. A multi-scale approach for simulating tidal marsh evolution. Ocean Dynam. **70**: 1187–1209.

Onitsuka, G., K. Miyahara, N. Hirose, S. Watanabe, H. Semura, R. Hori, T. Nishikawa, K. Miyaji, and M. Yamaguchi. 2010. Large-scale transport of *Cochlodinium polykrikoides* blooms by the Tsushima Warm Current in the southwest Sea of Japan. Harmful Algae **9**: 390–397.

Park, J. G., M. K. Jeong, J. A. Lee, K. J. Cho, and O. S. Kwon. 2001. Diurnal vertical migration of a harmful dinoflagellate, *Cochlodinium polykrikoides* (Dinophyceae), during a red tide in coastal waters of Namhae Island, Korea. Phycologia **40**: 292–297.

Pinto, L., M. Mateus, and A. Silva. 2016. Modeling the transport pathways of harmful algal blooms in the Iberian coast. Harmful Algae **53**: 8–16.

Qin, Q., and J. Shen. 2019. Physical transport processes affect the origins of harmful algal blooms in estuaries. Harmful Algae **84**: 210–221.

Qin, Q., J. Shen, K. S. Reece, and M. R. Mulholland. 2021. Developing a 3D mechanistic model for examining factors contributing to harmful blooms of *Margalefidinium polykrikoides* in a temperate estuary. Harmful Algae **105**: 102055.

Ralston, D. K., and S. K. Moore. 2020. Modeling harmful algal blooms in a changing climate. Harmful Algae **91**: 101729.

Roselli, L., M. R. Vadrucci, M. Belmonte, P. Ciciriello, F. Rubino, N. Ungaro, and C. Caroppo. 2020. Two-stages bloom of *Margalefidinium* cf. *polykrikoides* in a Mediterranean shallow bay (Ionian Sea, Italy). Mar. Pollut. Bull. **151**: 110825.

Shikata, T., and others. 2020. Vertical distribution of a harmful red-tide dinoflagellate, *Karenia mikimotoi*, at the decline stage of blooms. J. Sea Res. **165**: 101960.

Shulman, I., B. Penta, M. A. Moline, S. H. Haddock, S. Anderson, M. J. Oliver, and P. Sakalaukus. 2012. Can vertical migrations of dinoflagellates explain observed bioluminescence patterns during an upwelling event in Monterey Bay, California? J. Geophys. Res. Oceans **117**: C01016.

Sohn, M. H., K. W. Seo, Y. S. Choi, S. J. Lee, Y. S. Kang, and Y. S. Kang. 2011. Determination of the swimming trajectory and speed of chain-forming dinoflagellate *Cochlodinium polykrikoides* with digital holographic particle tracking velocimetry. Mar. Biol. **158**: 561–570.

Taylor, K. E. 2001. Summarizing multiple aspects of model performance in a single diagram. J. Geophys. Res. Atmos. **106**: 7183–7192.

Velo-Suárez, L., B. Reguera, S. González-Gil, M. Lunven, P. Lazure, E. Nézan, and P. Gentien. 2010. Application of a 3D Lagrangian model to explain the decline of a *Dinophysis acuminata* bloom in the Bay of Biscay. J. Mar. Syst. **83**: 242–252.

Weisberg, R. H., Y. Liu, C. Lembke, C. Hu, K. Hubbard, and M. Garrett. 2019. The coastal ocean circulation influence on the 2018 West Florida Shelf K. brevis red tide bloom. J. Geophys. Res. Oceans **124**: 2501–2512.

Wolny, J. L., M. C. Tomlinson, S. Schollaert Uz, T. A. Egerton, J. R. McKay, A. Meredith, K. S. Reece, G. P. Scott, and R. P. Stumpf. 2020. Current and future remote sensing of harmful algal blooms in the Chesapeake Bay to support the shellfish industry. Front. Mar. Sci. **7**: 337.

Wynne, T. T., R. P. Stumpf, M. C. Tomlinson, G. L. Fahnenstiel, J. Dyble, D. J. Schwab, and S. J. Joshi. 2013. Evolution of a cyanobacterial bloom forecast system in western Lake Erie: Development and initial evaluation. J. Great Lakes Res. **39**: 90–99.

Wynne, T. T., A. Meredith, R. Stumpf, T. Briggs, and W. Litaker. 2021. Harmful algal bloom forecasting branch ocean color satellite imagery processing guidelines, 2021 update. NOAA Technical Memorandum NOS NCCOS 296.48 doi:10.25923/606t-m243

Xiong, J., J. Shen, and Q. Wang. 2022. Storm-induced coastward expansion of *Margalefidinium polykrikoides* bloom in Chesapeake Bay. Mar. Pollut. Bull. **184**: 114187. doi:10.1016/j.marpolbul.2022.114187

Yñiguez, A. T., P. T. Lim, C. P. Leaw, S. J. Jipanin, M. Iwataki, G. Benico, and R. V. Azanza. 2021. Over 30 years of HABs in The Philippines and Malaysia: What have we learned? Harmful Algae **102**: 101776.

Yu, X., and J. Shen. 2021. A data-driven approach to simulate the spatiotemporal variations of chlorophyll-a in Chesapeake Bay. Ocean Model. **159**: 101748.

Zhang, Y., C. Chen, P. Xue, R. C. Beardsley, and P. J. Franks. 2020. A view of physical mechanisms for transporting harmful algal blooms to Massachusetts Bay. Mar. Pollut. Bull. **154**: 111048.

Zhang, Y. J., F. Ye, E. V. Stanev, and S. Grashorn. 2016. Seamless cross-scale modeling with SCHISM. Ocean Model. **102**: 64–81.

Zhou, F., J. Ge, D. Liu, P. Ding, C. Chen, and X. Wei. 2021. The Lagrangian-based Floating Macroalgal Growth and Drift Model (FMGDM v1. 0): Application to the Yellow Sea green tide. Geosci. Model Dev. **14**: 6049–6070.

Acknowledgments

The authors acknowledge William & Mary Research Computing (https://www.wm.edu/it/rc) for providing computational resources and technical support that have contributed to the results reported within this paper.

The authors thank Todd Egerton for providing cell abundance data of *M. polykrikoides*, Ross Vennell and Kimberly S. Reece for useful discussion in the model development, and Yizhen Li, Alexandria Hounshell, and Dongxiao Yin for proofreading the manuscript. Mulholland grants from NOAA ECOHAB, VDH, VA DEQ, and HRSD. We also appreciate the anonymous reviewers, the editor-in-chief, and the associated editor for their constructive suggestions and comments on the manuscript.

Submitted 30 May 2022
Revised 19 December 2022
Accepted 27 December 2022